

Original Research

# Texture Analysis as a Discriminating Tool: Unmasking Rodlet Cell Degranulation in Response to a Contaminant of Emerging Concern

Maurizio Manera<sup>1,\*</sup><sup>1</sup>Department of Biosciences, Food and Environmental Technologies, University of Teramo, 64100 Teramo, Italy\*Correspondence: [mmanera@unite.it](mailto:mmanera@unite.it) (Maurizio Manera)

Academic Editor: Gea Oliveri Conti

Submitted: 16 October 2023 Revised: 19 November 2023 Accepted: 29 November 2023 Published: 22 February 2024

## Abstract

**Background:** Contaminants of emerging concern (CECs) have garnered significant attention due to their potential impacts on ecology, wildlife, and human health. The interest in these contaminants arises from their inadequate regulation or lack of routine monitoring in natural environments. Among them, per- and polyfluoroalkyl substances (PFAS) are of particular concern due to their notable propensity to accumulate within the kidney, significantly influencing the excretion of these pollutants. Rodlet cells (RCs) have emerged as promising indicators of immunotoxicity in response to chemical stressors. A prior comprehensive study extensively detailed the effects of sub-chronic exposure to perfluorooctanoic acid (PFOA), a well-known PFAS compound, on RCs located in the hematopoietic tissue of the common carp kidney. Even at concentrations commonly found in the environment, PFOA exhibited a significant impact on the distribution patterns of RCs, concurrently enhancing exocytosis activity. **Methods:** The assessment of PFOA-induced RC degranulation employed texture analysis combined with linear discriminant analysis (LDA) to differentiate between various experimental exposure groups. The investigation encompassed three fish groups: an unexposed group, a group exposed to an environmentally relevant PFOA concentration (200 ng L<sup>-1</sup>), and a group exposed to a higher PFOA concentration (2 mg L<sup>-1</sup>). Texture analysis was conducted on high-resolution color (RGB) images obtained from light microscopy of ultrathin sections from five fish per experimental group, stained with toluidine blue. **Results:** This analysis facilitated the quantification of potential cytoplasmic alterations associated with degranulation, encompassing all three RGB channels. The data subjected to LDA enabled the identification of the most distinctive texture characteristics, providing a reliable, objective, and reproducible method to differentiate between experimental groups. Remarkably, 98.0% of both the original and cross-validated cases were correctly classified. However, only one unexposed case was misclassified as a fish exposed to a 200 ng L<sup>-1</sup> PFOA concentration, constituting the single false positive in the analysis. **Conclusions:** Utilizing texture analysis and LDA to quantify RC degranulation offers a dependable approach for assessing immunotoxicity within experimental models of toxicological and environmental pathology. This underscores the scientific significance of employing a morphological approach in such investigations.

**Keywords:** image analysis; linear discriminant analysis; fish model; common carp; PFAS; immunotoxicity; degranulation patterns; toxicologic pathology; environmental pathology

## 1. Introduction

Contaminants of emerging concern (CECs) hold a paramount position in the realm of environmental science due to their potential ecological, wildlife, and human health implications, primarily stemming from their limited regulation and insufficient routine monitoring within natural environments [1]. Among the significant categories of CECs, per- and polyfluoroalkyl substances (PFAS) emerge as a central concern [2]. These substances can accumulate in renal tissues at substantial concentrations, prominently influencing their excretory function and manifesting potential nephrotoxicity [3–6]. Furthermore, PFAS compounds have been recognized for their immunotoxic effects [7–9].

Perfluorooctanoic acid (PFOA), a well-known member of the PFAS group, is characterized by its amphiphilic nature, featuring a hydrophobic seven-carbon chain with fluorine atom substitutions for hydrogen and a hydrophilic carboxylic group [10]. Its exceptional solubility in wa-

ter, recalcitrance, and prolonged half-lives within biological systems have raised considerable concerns in aquatic ecosystems [11,12].

Fish, as a crucial component of aquatic ecosystems, experience consistent exposure to PFOA, resulting in its bioaccumulation within their tissues [13,14]. This situation raises concerns about potential human exposure to PFOA through the consumption of fish within the food supply chain [15]. Therefore, fish species serve as valuable subjects for researching the toxicologic and environmental pathologic effects of PFOA according to the holistic One Health perspective [16,17].

Although research on PFOA effects has largely focused on cyprinids like zebrafish (*Danio rerio*) [18], the common carp (*Cyprinus carpio*) stands as a robust model for studying the impact of this pollutant on fish communities in nature. Its availability for research, ease of maintenance, significance as a food source, abundance in freshwater ecosystems, and role as an “ecological engineer”



[19] make it an ideal candidate for assessing emerging pollutants' effects. Its effectiveness has been demonstrated in both experimental and field research concerning PFAS compounds [5,7,8,20–22].

The common carp's kidney, comprising various histological components such as nephrons, hematopoietic tissue, and thyroid follicles [23], has garnered attention as a versatile and multipurpose biomarker organ. This recognition extends to its relevance in environmental pathology, toxicological research, and translational medicine due to its potential to assess the impacts of toxic exposures on various functionalities [5,7,8,22].

Rodlet cells (RCs), a unique feature found in teleosts, were initially documented by Thélohan in 1892. Subsequent to this discovery, extensive literature reviews have examined the characteristics, origin, structure, and functionality of these distinct cells. These studies highlight their potential as biomarkers for chemical exposure [24,25]. RCs primarily reside in the epithelia of various organs in fish species from both freshwater and saltwater habitats [24,25]. Morphologically, mature RCs exhibit a distinct polarized profile, featuring a peripheral cytoplasmic area with aligned microfilaments, rod-shaped granules known as rodlets, and the remaining section of the cytoplasm displaying conspicuous vesiculations. Furthermore, the nucleus is positioned at one extremity [8,24,25].

In recent decades, mounting evidence has highlighted the integral role of RCs in the innate immune system of fish, demonstrating their capacity to respond to different noxae [7,8,24,26–28]. This assertion finds support in various aspects: First, the resemblance and shared features observed between RCs and leukocytes, notably their perivascular positioning and the presence of villous projections, which exhibit structural similarities, potentially resembling T cell microvilli [8,25,29,30]. Second, RCs demonstrate aggregation at sites affected by both micro- and macroparasites [25,31]. Third, RCs exhibit close associations with other immune cells [7,24,29]. Fourth, the immunolocalization of immune-active components within RCs, such as tumor necrosis factor  $\alpha$ , lysozyme, inducible nitric oxide synthase, and piscidin 1 [28,32,33], along with Toll-like receptor-2 [34], further underscores their involvement in immune responses.

RCs were shown to react to diverse noxae, encompassing parasites and environmental pollutants, showcasing alterations in their cellular functions, including secretion patterns and recruitment [7,8,31]. Recent studies have highlighted the potential of RCs to serve as valuable biomarkers for evaluating immunotoxicity resulting from exposure to chemical stressors [7,8].

In a previous study involving fish from the same experimental cohort as the present research, an investigation was conducted to assess the effects of varying concentrations of PFOA. This analysis encompassed a comprehensive evaluation utilizing both structural and ultra-

structural methodologies to examine the distribution of RCs within the tissue and their exocytosis patterns. Additionally, quantitative assessment through biometric analysis was employed to determine the abundance of RCs within the hematopoietic tissue [8]. The outcomes of that investigation demonstrated that PFOA exerted a significant influence on the distribution patterns of RC. This held true even at a 200 ng L<sup>-1</sup> PFOA concentration—an environmentally relevant concentration [8]. This influence was characterized by an increase in the prevalence of RCs and their tendency to aggregate, along with heightened exocytosis (degranulation) activity. The latter activity was qualitatively characterized both structurally and ultrastructurally and was found to be correlated with PFOA concentration.

These findings elucidate the immunotoxic effects of PFOA on fish and imply the potential of RCs to serve as sentinel cells in responding to environmental pollutants within the immune system [8].

The term “texture” encompasses various patterns and sub-patterns of brightness, color, and other visual attributes [35,36]. The initial step in image texture analysis involves feature extraction, which quantitatively describes the texture using structural, statistical, model-based, and transformation-based methods [35–37]. Subsequently, the objective is texture discrimination, with the goal of identifying and categorizing image regions with consistent texture properties, such as distinguishing between normal and pathological areas [37,38].

In the context of this study, the primary objective is to provide a quantitative characterization of PFOA-induced degranulation within RCs in common carp exposed to an environmentally relevant PFOA concentration (200 ng L<sup>-1</sup>), and a higher PFOA concentration (2 mg L<sup>-1</sup>). This characterization is achieved through a comprehensive analysis of the texture of RC cytoplasm, coupled with the application of linear discriminant analysis (LDA). This integrated approach provides an objective and replicable method for discerning the extent of degranulation across different experimental groups, thereby eliminating potential operator-dependent biases. Notably, the combined use of texture analysis and LDA has previously demonstrated its efficacy in the reliable quantitative characterization of mast cell degranulation in fish [39–41].

## 2. Materials and Methods

### 2.1 Experimental Design

The kidney specimens used in this investigation were derived from a previous study conducted by Giari *et al.* (2016) [42]. While a summarized version is presented here, detailed information regarding fish selection, maintenance, and the specific experimental framework concerning PFOA exposure is available in the aforementioned publication. Thirty-one adult common carp (*Cyprinus carpio*), two years old, were obtained from a local fish farm and acclimatized over a four-week period. Throughout the exposure test,

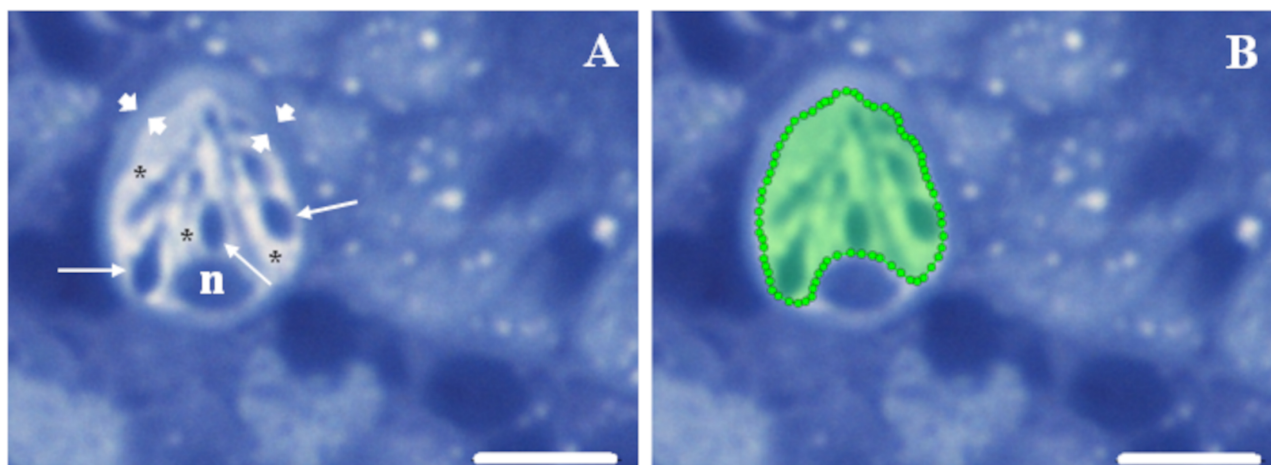


**Fig. 1. Region of interest selection procedure.** (A) The peculiar structural features of mature rodlet cells facilitate their detection within the hematopoietic tissue. Key features include a polarized pear shape with the nucleus (n) located at one extremity, typical rod-shaped granules, the so-named rodlets (thin arrows), pointing towards the opposite extremity, and a notable peripheral thickening of the cytoplasm, resembling a “capsule” (arrowheads). These features are easily visible, along with the vesiculated aspect (asterisks) of the rest of the cytoplasm, which is enhanced by perfluorooctanoic acid (PFOA) exposure. (B) A region of interest (ROI) can be easily delineated using the polygon selection tools in Icy, with the “capsule” serving as a guide to encompass the cytoplasm while excluding the nucleus. Semithin kidney sections from a fish exposed to  $2 \text{ mg L}^{-1}$  PFOA, stained with toluidine blue. Scale bar =  $10 \text{ }\mu\text{m}$ .

these specimens were maintained under a 14:10 h light–dark cycle and fed thrice weekly with pellet food (Tetra Pond Pellets Mini, Tetra, Melle, Germany). The subjects were divided into three groups: a control group unexposed to PFOA ( $n = 10$ ), a group exposed to an environmentally relevant PFOA concentration ( $200 \text{ ng L}^{-1}$ ) ( $n = 10$ ), and a group exposed to a higher PFOA concentration ( $2 \text{ mg L}^{-1}$ ) ( $n = 11$ ). Each cohort was housed in a 120 L glass aquarium supplied with tap water, receiving a constant fresh water supply (flow-through rate of  $500 \text{ mL min}^{-1}$ ). PFOA was consistently delivered into two treatment aquaria through a peristaltic pump to achieve specified concentrations. The  $200 \text{ ng L}^{-1}$  concentration emulated an environmentally relevant level observed in surface water, while the  $2 \text{ mg L}^{-1}$  concentration was based on evidence known to provoke histological responses in cyprinid fish [8,42]. Monitoring of key parameters such as water temperature ( $10\text{--}15 \text{ }^\circ\text{C}$ ), pH ( $6.70\text{--}8.00$ ), and oxygen saturation ( $>80\%$ ) occurred three times a week in each aquarium. After a 56-day sub-chronic exposure period, humane euthanasia was performed using tricaine methane-sulfonate (MS-222), followed by necropsies.

## 2.2 Tissue Processing

In the current investigation, 15 representative kidney specimens were collected from 15 common carp, comprising 5 samples each from unexposed carp, carp exposed to an environmentally relevant PFOA concentration ( $200 \text{ ng L}^{-1}$ ), and carp exposed to a higher PFOA concentration ( $2 \text{ mg L}^{-1}$ ). The kidney samples underwent standard electron microscopy preparation. Initially, they were fixed in a 2.5%

glutaraldehyde-buffered solution (sodium cacodylate, pH 7.3) for 3 hours at  $4 \text{ }^\circ\text{C}$ . Subsequently, a 1% osmium tetroxide solution was applied for 2 hours. Dehydration using acetone followed the fixation. Embedding in epoxy resin (Durcupan™ ACM, Fluka, Sigma-Aldrich, St. Louis, MO, USA) and sectioning with a Reichert Om U2 ultramicrotome (Reichert-Jung Co., Heidelberg, Germany) produced approximately  $90 \text{ nm}$  thick ultrathin sections. These sections were stained with toluidine blue for examination and imaging using a Nikon Eclipse 80i light microscope (Nikon, Tokyo, Japan) equipped with a digital camera.

## 2.3 Texture Analysis

High-resolution color (RGB) images with dimensions of  $2560 \times 1920$  pixels ( $20 \text{ pixels} = 1 \text{ }\mu\text{m}$ ) were employed for image analysis at a magnification of  $1000\times$ . The distinctive morphology of RCs (Fig. 1A) facilitated their easy identification within the hematopoietic tissue. The cytoplasm of RCs, sectioned along their main axis, was selected using polygon selection tools in Icy software (version 2.4.3.0, Institut Pasteur and France BioImaging, Paris and Montpellier, France), as illustrated in Fig. 1B. Subsequently, the following texture features were extracted from the selected region of interest (ROI) for each of the color RGB channels, utilizing the ROI statistics tool in Icy:

- For the first-order texture analysis method, grey-level histogram analysis was employed, resulting in the following features: minimal intensity, mean intensity, maximal intensity, sum intensity, and standard deviation.
- For the second-order texture analysis method, analysis of the grey-level co-occurrence matrix (GLCM) was

## Canonical Discriminant Functions

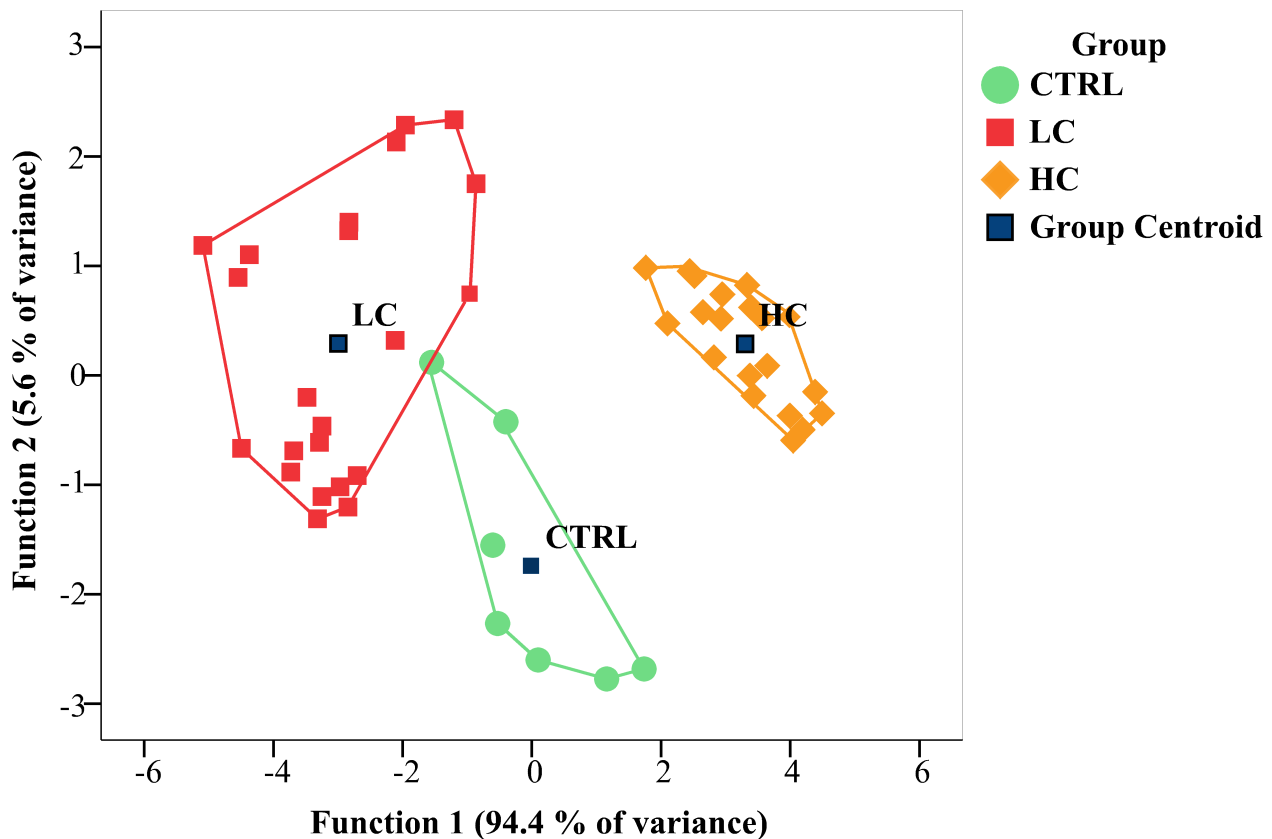


**Fig. 2. Canonical discriminant function plot.** Group centroids are represented as black squares. Individual samples, representing the cytoplasm screened for texture features from each rodlet cell (RC), are indicated using distinct symbols and colors, corresponding to their respective experimental groups. Notably, the unexposed group's convex hull partially overlaps with that of the 200 ng L<sup>-1</sup> PFOA group, signifying a single misclassified case (false positive). In contrast, cases from the 2 mg L<sup>-1</sup> PFOA group appear to be distinctly discriminated along the primary discriminant axis (discriminant function 1), accounting for 94.4% of the variance explained by the model. Ctrl, unexposed; LC, 200 ng L<sup>-1</sup> PFOA; HC, 2 mg L<sup>-1</sup> PFOA.

conducted, yielding Haralick's texture features: texture angular second moment, texture contrast, texture entropy, and texture homogeneity.

The selection of both first-order and second-order texture analysis methods was based on their complementary nature and their ability to provide comprehensive insights into cell degranulation, as reported in previous research [39–41].

### 2.4 Statistical Analysis

Texture feature datasets underwent assessment for normal distribution and equality of variance using the Shapiro–Wilk test and Levene test, respectively. Subsequently, these features underwent linear discriminant analysis (LDA), stepwise analysis, and Mahalanobis distance using SPSS 14.0.2 (SPSS Inc., Chicago, IL, USA). LDA relies on the categorization of data into different classes or

groups. By categorizing data, LDA can identify the most discriminative features or dimensions that separate these categories, leading to more accurate and efficient classification results [43]. Given that some texture features exhibited slight deviations from normality and/or homogeneity of variance, it's worth noting that LDA is generally considered robust enough to accommodate such deviations. However, as a precaution, the dataset was reevaluated and confirmed following normalization transformations (including square-root and logarithmic transformations). Additionally, both a pooled covariance matrix and separate covariance matrices were employed, as suggested by Norušis (2005) [43].

## 3. Results

The outcomes of the LDA applied to texture features are summarized visually in Fig. 2 and detailed in Tables 1–3. These tables present classification results for both

**Table 1. Variables in the analysis.**

Step		Tolerance	F-to-Remove	Min. D Squared	Between Groups
1	Max Intensity (ch 1)	1.000	10.340		
2	Max Intensity (ch 1)	0.263	35.547	0.005	Ctrl and HD
	Max Intensity (ch 2)	0.263	71.044	0.190	LD and HD
3	Max Intensity (ch 1)	0.259	15.230	3.895	Ctrl and HD
	Max Intensity (ch 2)	0.249	54.387	3.145	LD and HD
	Mean Intensity (ch 1)	0.684	8.405	4.865	Ctrl and LD
4	Max Intensity (ch 1)	0.225	7.323	8.835	Ctrl and HD
	Max Intensity (ch 2)	0.217	59.681	3.246	Ctrl and HD
	Mean Intensity (ch 1)	0.485	17.692	6.478	Ctrl and LD
	Standard Deviation (ch 1)	0.396	11.580	5.939	Ctrl and LD
5	Max Intensity (ch 1)	0.215	7.485	9.253	Ctrl and HD
	Max Intensity (ch 2)	0.188	70.323	3.264	Ctrl and HD
	Mean Intensity (ch 1)	0.452	20.063	7.376	Ctrl and LD
	Standard Deviation (ch 1)	0.130	14.977	6.742	Ctrl and LD
	Texture contrast (ch 0)	0.187	4.261	10.651	Ctrl and LD

In this table, the variables retained at each step of the analysis, as determined through stepwise analysis and Mahalanobis distance, are presented. The table also includes the F value for the change in Wilk's lambda. The default values for F-to-enter and F-to-remove are set at 3.84 and 2.71, respectively. Ctrl signifies the control group without exposure to perfluorooctanoic acid (PFOA), LD denotes the low dosage group (200 ng L<sup>-1</sup> PFOA), and HD designates the high dosage group (2 mg L<sup>-1</sup> PFOA).

the original and cross-validated cases. The LDA method achieved 98% accuracy in correctly classifying cases, with only one false positive instance. Specifically, one unexposed case was misclassified as exposed to 200 ng L<sup>-1</sup> PFOA. In terms of the diagnostic properties, considering unexposed fish as negative cases and exposed fish as positive cases, the following key properties were preserved: diagnostic sensitivity of 100%, diagnostic specificity of 86%, diagnostic accuracy of 98%, predictive value of a positive test of 98%, and predictive value of a negative test of 100%. These results held consistent across original cases, cross-validated cases, and jackknifed resampled cases. It's noteworthy that jackknife resampling was performed using separate software (Past 4.14; Øyvind Hammer, Natural History Museum, University of Oslo, Oslo, Norway).

#### 4. Discussion

The exploration of RC degranulation in response to toxic exposure remains relatively unexplored in the scientific literature, barring a prior qualitative structural and ultrastructural study conducted in carp from the current experimental cohort [8]. This earlier investigation specifically examined RC distribution and exocytosis patterns using light and transmission electron microscopy, along with biometric measurements quantifying RCs within the hematopoietic tissue [8]. The findings from that study revealed that even at a concentration as low as 200 ng L<sup>-1</sup>, considered environmentally relevant, PFOA significantly influenced RC distribution patterns. Specifically, exposure to PFOA led to increased cluster formation and height-

ened exocytosis activity. These observations underscore the immunotoxic effects of this pollutant in fish and suggest the potential of RCs to act as sentinel cells within the immune system, responding to environmental pollutants [8]. Examination under light microscopy revealed that RCs from PFOA-exposed fish displayed heightened cytoplasmic vesiculation, leading to enhanced visual clarity compared to RCs from the unexposed group. Furthermore, the exposed samples showed a higher occurrence of discharging or discharged RCs [8]. The ultrastructural analysis revealed heightened dissolution of rodlet sacs and increased fusion of rodlet membranes in PFOA-exposed fish. Additionally, there was a significant enhancement in the protrusion and fusion of cytoplasmic vesicles, both within and with adjacent ones [8]. These structural alterations collectively contributed to the clearer and more vesicle-rich appearance of RCs observed under light microscopy [8]. These findings confirmed the intrinsic exocytosis activity of RCs, known for piecemeal exocytosis. Furthermore, they underscored that exposure to PFOA amplifies this basal exocytosis activity in a concentration-dependent manner, leading to enhanced fusion of rodlet membranes, akin to the process observed in compound exocytosis [8].

In the present investigation, the aforementioned qualitative findings were validated through an objective approach utilizing texture analysis of cytoplasm and subsequent statistical analysis employing LDA. The grayscale variations from all three RGB channels, represented by the most discriminatory texture features, effectively summarized the structural and ultrastructural variations among

**Table 2. Pairwise group comparisons<sup>a,b,c,d,e</sup>.**

Step	Group		Unexposed	200 ng L <sup>-1</sup> PFOA	2 mg L <sup>-1</sup> PFOA
1	Unexposed	F		20.662	12.237
		Sig.		0.000	0.001
	200 ng L <sup>-1</sup> PFOA	F	20.662		1.994
		Sig.	0.000		0.165
	2 mg L <sup>-1</sup> PFOA	F	12.237	1.994	
		Sig.	0.001	0.165	
2	Unexposed	F		12.638	24.543
		Sig.		0.000	0.000
	200 ng L <sup>-1</sup> PFOA	F	12.638		70.832
		Sig.	0.000		0.000
	2 mg L <sup>-1</sup> PFOA	F	24.543	70.832	
		Sig.	0.000	0.000	
3	Unexposed	F		10.055	20.230
		Sig.		0.000	0.000
	200 ng L <sup>-1</sup> PFOA	F	10.055		69.378
		Sig.	0.000		0.000
	2 mg L <sup>-1</sup> PFOA	F	20.230	69.378	
		Sig.	0.000	0.000	
4	Unexposed	F		13.218	16.727
		Sig.		0.000	0.000
	200 ng L <sup>-1</sup> PFOA	F	13.218		79.531
		Sig.	0.000		0.000
	2 mg L <sup>-1</sup> PFOA	F	16.727	79.531	
		Sig.	0.000	0.000	
5	Unexposed	F		12.621	14.295
		Sig.		0.000	0.000
	200 ng L <sup>-1</sup> PFOA	F	12.621		75.835
		Sig.	0.000		0.000
	2 mg L <sup>-1</sup> PFOA	F	14.295	75.835	
		Sig.	0.000	0.000	

<sup>a</sup>1, 46 degrees of freedom for step 1.

<sup>b</sup>2, 45 degrees of freedom for step 2.

<sup>c</sup>3, 44 degrees of freedom for step 3.

<sup>d</sup>4, 43 degrees of freedom for step 4.

<sup>e</sup>5, 42 degrees of freedom for step 5.

The pairwise group comparison at each step during the stepwise analysis is reported, showing the improvement in discrimination at each step. PFOA, perfluorooctanoic acid.

the experimental groups, as documented in the preceding study [8]. More specifically, the ultrastructural changes induced by PFOA in RC cytoplasm, which manifest as the clearer and more vesiculated aspect observable under light microscopy, gave rise to a distinctive grayscale distribution pattern, commonly referred to as texture. This texture pattern was unique to each experimental group and served as a reliable discriminative feature among them.

As previously mentioned, the fish in this study were derived from a prior experimental cohort that used toluidine blue as the staining method for ultrathin sections. Intriguingly, despite the application of a predominantly monochromatic stain, all three RGB channels contributed to the dis-

crimination among experimental groups, suggesting potential avenues for further research involving polychromatic staining techniques and/or testing across multiple wavelengths spanning a wide spectral range, as seen in hyperspectral microscopy. Nevertheless, it is imperative to emphasize that the primary objective of this study was not to identify absolute discriminant values for use as reference points. Rather, it aimed to propose a dependable and objective method for comparing samples against a known control, facilitating the objective characterization of changes induced by degranulation in RC cytoplasm, to be used in toxicologic and environmental pathology studies.

**Table 3. Classification results<sup>b,c</sup> according to Mahalanobis distance stepwise method.**

Group		Predicted Group Membership			Total	
		Unexposed	200 ng L <sup>-1</sup> PFOA	2 mg L <sup>-1</sup> PFOA		
Original	Count	Unexposed	6	1	0	7
		200 ng L <sup>-1</sup> PFOA	0	22	0	22
		2 mg L <sup>-1</sup> PFOA	0	0	20	20
	%	Unexposed	85.7	14.3	0.0	100.0
		200 ng L <sup>-1</sup> PFOA	0.0	100.0	0.0	100.0
		2 mg L <sup>-1</sup> PFOA	0.0	0.0	100.0	100.0
Cross-validated <sup>a</sup>	Count	Unexposed	6	1	0	7
		200 ng L <sup>-1</sup> PFOA	0	22	0	22
		2 mg L <sup>-1</sup> PFOA	0	0	20	20
	%	Unexposed	85.7	14.3	0.0	100.0
		200 ng L <sup>-1</sup> PFOA	0.0	100.0	0.0	100.0
		2 mg L <sup>-1</sup> PFOA	0.0	0.0	100.0	100.0

<sup>a</sup>Cross validation is carried out only for those cases in the analysis. In cross validation, each case is classified by the functions derived from all cases other than that case.

<sup>b</sup>98% of originally grouped cases correctly classified.

<sup>c</sup>98% of cross-validated grouped cases correctly classified.

In this table, the classification results achieved through the Mahalanobis distance stepwise method are presented. The results demonstrate a 98% correct classification rate for both original and cross-validated cases, with only one false positive case. Specifically, an unexposed case was misclassified as exposed to 200 ng L<sup>-1</sup> PFOA.

RCs have been acknowledged as essential components of the fish's innate immune system, as evidenced by previous studies [7,24,27,28]. Furthermore, degranulation of RCs has been observed in association with various noxious agents, including toxic substances [7,8,44,45]. As degranulation is a crucial mechanism through which immune cells interact with their environment, encompassing host cells, tissues, and pathogens [46], its induction by toxics deserves considerable attention, especially concerning its potential impact on immunocompetence [7,8]. This underscores the importance of employing reliable tools to assess RC degranulation. Notably, texture analysis and LDA have previously demonstrated their effectiveness in characterizing mast cell degranulation in fish [39–41].

## 5. Conclusions

In conclusion, this study has focused on exploring RC degranulation in response to PFOA exposure, employing texture analysis in combination with LDA to objectively characterize grayscale differences in RC cytoplasm among experimental groups. The quantitative analyses conducted have demonstrated the efficacy of these methods in discerning subtle changes induced by RC degranulation due to PFOA exposure.

Significantly, the findings underscore the unique capability of LDA in distinguishing among experimental groups based on distinctive texture features derived from RC cytoplasm. These observations highlight discernible variations in RC characteristics consequent to PFOA exposure, aligning with known immunotoxic effects associated with such contaminants.

The results of this study suggest that texture analysis coupled with LDA serves as a powerful tool for objectively assessing contaminant-induced alterations in cellular structures. By providing insights into immunotoxicity mechanisms, this research potentially contributes to the development of robust methodologies applicable to toxicological and environmental pathology research.

Ultimately, this research has the potential to impact public health policies by enhancing the ability to objectively evaluate the effects of environmental contaminants on cellular morphology, thereby contributing significantly to the broader field of environmental health and toxicology.

## Availability of Data and Materials

The datasets used and/or analyzed during the current study are available from the corresponding author on reasonable request.

## Author Contributions

The single author had the sole role in designing, data collecting, analyzing, and writing the manuscript. MM read and approved the final manuscript. MM has participated sufficiently in the work and agreed to be accountable for all aspects of the work.

## Ethics Approval and Consent to Participate

Not applicable, as fish samples were sourced from a prior experiment [42], adhering to the Italian regulations for animal research in place at that time, with a primary aim of reducing suffering, stress, and discomfort. Consequently, no fish were deliberately sacrificed for the present study.

## Acknowledgment

The author is grateful to Luisa Giari for technical help.

## Funding

This research received no external funding.

## Conflict of Interest

The author declares no conflict of interest. Given the role as Guest Editor, Maurizio Manera had no involvement in the peer-review of this article and has no access to information regarding its peer-review. Full responsibility for the editorial process for this article was delegated to Gea Oliveri Conti.

## References

- [1] Ankley GT, Bennett R, Erickson RJ, Hoff DJ, Mount DR, Tietge J, *et al.* Aquatic Life Criteria for Contaminants of Emerging Concern. 2008. Available at: [https://www.epa.gov/sites/default/files/2015-08/documents/white\\_paper\\_aquatic\\_life\\_criteria\\_for\\_contaminants\\_of\\_emerging\\_concern\\_part\\_i\\_general\\_challenges\\_and\\_recommendations\\_1.pdf](https://www.epa.gov/sites/default/files/2015-08/documents/white_paper_aquatic_life_criteria_for_contaminants_of_emerging_concern_part_i_general_challenges_and_recommendations_1.pdf) (Accessed: 19 November 2023).
- [2] Podder A, Sadmani AHMA, Reinhart D, Chang NB, Goel R. Per and poly-fluoroalkyl substances (PFAS) as a contaminant of emerging concern in surface water: A transboundary review of their occurrences and toxicity effects. *Journal of Hazardous Materials.* 2021; 419: 126361.
- [3] Fenton SE, Ducatman A, Boobis A, DeWitt JC, Lau C, Ng C, *et al.* Per- and Polyfluoroalkyl Substance Toxicity and Human Health Review: Current State of Knowledge and Strategies for Informing Future Research. *Environmental Toxicology and Chemistry.* 2021; 40: 606–630.
- [4] Buser M, Jones D, Pohl HR, Ruiz P, Scinicariello F, Chou S, *et al.* Toxicological Profile for Perfluoroalkyls. 2021. Available at: <https://www.atsdr.cdc.gov/toxprofiles/tp200.pdf> (Accessed: 19 November 2023).
- [5] Manera M, Casciano F, Giari L. Ultrastructural Alterations of the Glomerular Filtration Barrier in Fish Experimentally Exposed to Perfluorooctanoic Acid. *International Journal of Environmental Research and Public Health.* 2023; 20: 5253.
- [6] Kudo N, Kawashima Y. Toxicity and toxicokinetics of perfluorooctanoic acid in humans and animals. *The Journal of Toxicological Sciences.* 2003; 28: 49–57.
- [7] Manera M, Castaldelli G, Guerranti C, Giari L. Effect of waterborne exposure to perfluorooctanoic acid on nephron and renal hemopoietic tissue of common carp *Cyprinus carpio*. *Ecotoxicology and Environmental Safety.* 2022; 234: 113407.
- [8] Manera M, Castaldelli G, Giari L. Perfluorooctanoic Acid Promotes Recruitment and Exocytosis of Rodlet Cells in the Renal Hematopoietic Tissue of Common Carp. *Toxics.* 2023; 11: 831.
- [9] Liang L, Pan Y, Bin L, Liu Y, Huang W, Li R, *et al.* Immunotoxicity mechanisms of perfluorinated compounds PFOA and PFOS. *Chemosphere.* 2022; 291: 132892.
- [10] Mokra K. Endocrine Disruptor Potential of Short- and Long-Chain Perfluoroalkyl Substances (PFASs)-A Synthesis of Current Knowledge with Proposal of Molecular Mechanism. *International Journal of Molecular Sciences.* 2021; 22: 2148.
- [11] EFSA Panel on Contaminants in the Food Chain (EFSA CONTAM Panel), Schrenk D, Bignami M, Bodin L, Chipman JK, Del Mazo J, *et al.* Risk to human health related to the presence of perfluoroalkyl substances in food. *EFSA Journal.* European Food Safety Authority. 2020; 18: e06223.
- [12] Abunada Z, Alazaiza MYD, Bashir MJK. An overview of per- and polyfluoroalkyl substances (Pfas) in the environment: Source, fate, risk and regulations. *Water.* 2020; 12: 3590.
- [13] Lee JW, Choi K, Park K, Seong C, Yu SD, Kim P. Adverse effects of perfluoroalkyl acids on fish and other aquatic organisms: A review. *The Science of the Total Environment.* 2020; 707: 135334.
- [14] Du D, Lu Y, Zhou Y, Li Q, Zhang M, Han G, *et al.* Bioaccumulation, trophic transfer and biomagnification of perfluoroalkyl acids (PFAAs) in the marine food web of the South China Sea. *Journal of Hazardous Materials.* 2021; 405: 124681.
- [15] Sunderland EM, Hu XC, Dassuncao C, Tokranov AK, Wagner CC, Allen JG. A review of the pathways of human exposure to poly- and perfluoroalkyl substances (PFASs) and present understanding of health effects. *Journal of Exposure Science & Environmental Epidemiology.* 2019; 29: 131–147.
- [16] Haschek WM, Rousseaux CG, Wallig MA. *Toxicologic Pathology: An Introduction.* In Haschek WM, Rousseaux CG, Wallig MA (eds) *Haschek and Rousseaux's Handbook of Toxicologic Pathology.* 3rd edn. Academic Press: San Diego, CA. 2013.
- [17] Friese C, Nuyts N. Posthumanist critique and human health: how nonhumans (could) figure in public health research. *Crit Public Health.* 2017; 27: 303–313.
- [18] Ankley GT, Cureton P, Hoke RA, Houde M, Kumar A, Kurias J, *et al.* Assessing the Ecological Risks of Per- and Polyfluoroalkyl Substances: Current State-of-the Science and a Proposed Path Forward. *Environmental Toxicology and Chemistry.* 2021; 40: 564–605.
- [19] Rahman MM. Role of common carp (*Cyprinus carpio*) in aquaculture production systems. *Frontiers in Life Science.* 2015; 8: 399–410.
- [20] Kim WK, Lee SK, Jung J. Integrated assessment of biomarker responses in common carp (*Cyprinus carpio*) exposed to perfluorinated organic compounds. *Journal of Hazardous Materials.* 2010; 180: 395–400.
- [21] Ye X, Schoenfuss HL, Jahns ND, Delinsky AD, Strynar MJ, Varns J, *et al.* Perfluorinated compounds in common carp (*Cyprinus carpio*) filets from the Upper Mississippi River. *Environment International.* 2008; 34: 932–938.
- [22] Manera M, Castaldelli G, Giari L. Perfluorooctanoic Acid Affects Thyroid Follicles in Common Carp (*Cyprinus carpio*). *International Journal of Environmental Research and Public Health.* 2022; 19: 9049.
- [23] Geven EJW, Klaren PHM. The teleost head kidney: Integrating thyroid and immune signalling. *Developmental and Comparative Immunology.* 2017; 66: 73–83.
- [24] Manera M, Dezfuli BS. Rodlet cells in teleosts: a new insight into their nature and functions. *Journal of Fish Biology.* 2004; 65:597–619.
- [25] Sayyaf Dezfuli B, Pironi F, Maynard B, Simoni E, Bosi G. Rodlet cells, fish immune cells and a sentinel of parasitic harm in teleost organs. *Fish & Shellfish Immunology.* 2022; 121: 516–534.
- [26] Reite OB. Mast cells/eosinophilic granule cells of salmonids: staining properties and responses to noxious agents. *Fish Shellfish Immunol.* 1997; 7: 567–584.
- [27] Reite OB. The rodlet cells of teleostean fish: their potential role in host defence in relation to the role of mast cells/eosinophilic granule cells. *Fish & Shellfish Immunology.* 2005; 19: 253–267.
- [28] Bosi G, DePasquale JA, Manera M, Castaldelli G, Giari L, Sayyaf Dezfuli B. Histochemical and immunohistochemical characterization of rodlet cells in the intestine of two teleosts, *Anguilla anguilla* and *Cyprinus carpio*. *Journal of Fish Diseases.* 2018; 41: 475–485.
- [29] Manera M, Simoni E, Dezfuli BSS. The effect of dexamethasone on the occurrence and ultrastructure of rodlet cells in goldfish. *Journal of Fish Biology.* 2001; 59: 1239–1248.

- [30] Smith SA, Caceci T, Marei HE, El-Haback HA. Observations on rodlet cells found in the vascular system and extravascular space of angelfish (*Pterophyllum scalare scalare*). *Journal of Fish Biology*. 1995; 46: 241–254.
- [31] Dezfuli BS, Bosi G, DePasquale JA, Manera M, Giari L. Fish innate immunity against intestinal helminths. *Fish & Shellfish Immunology*. 2016; 50: 274–287.
- [32] Silphaduang U, Colomi A, Noga EJ. Evidence for widespread distribution of piscidin antimicrobial peptides in teleost fish. *Diseases of Aquatic Organisms*. 2006; 72: 241–252.
- [33] Ronza P, Losada AP, Villamarín A, Bermúdez R, Quiroga MI. Immunolocalization of tumor necrosis factor alpha in turbot (*Scophthalmus maximus*, L.) tissues. *Fish & Shellfish Immunology*. 2015; 45: 470–476.
- [34] Alesci A, Pergolizzi S, Capillo G, Lo Cascio P, Lauriano ER. Rodlet cells in kidney of goldfish (*Carassius auratus*, Linnaeus 1758): A light and confocal microscopy study. *Acta Histochemica*. 2022; 124: 151876.
- [35] Haralick RM, Shanmugam K, Dinstein I. Textural features for image classification. *IEEE Trans Syst Man Cybern*. 1973; 3: 610–621.
- [36] Haralick RM, Shapiro LG. Image Segmentation Techniques. *Comput Vision, Graph Image Process*. 1985; 29: 100–132.
- [37] Materka A, Strzelecki M. Texture Analysis Methods – A Review. COST B11 report. 1998. Available at: [http://www.eletel.p.lodz.pl/programy/cost/pdf\\_1.pdf](http://www.eletel.p.lodz.pl/programy/cost/pdf_1.pdf) (Accessed: 10 June 2016).
- [38] Szczyppinski PM, Strzelecki M, Materka A. MaZda - a Software for Texture Analysis. 2007 International Symposium on Information Technology Convergence. Jeonju, Korea. 2007.
- [39] Manera M, Borreca C. Assessment of mast cells degranulation in rainbow trout (*Oncorhynchus mykiss* Walbaum) by means of gray level and texture analysis (Gray Level Correlation Matrices). *Research in Veterinary Science*. 2012; 93: 886–891.
- [40] Manera M. The Use of texture analysis in the morpho-functional characterization of mast cell degranulation in rainbow trout (*Oncorhynchus mykiss*). *Microscopy and Microanalysis: the Official Journal of Microscopy Society of America, Microbeam Analysis Society, Microscopical Society of Canada*. 2013; 19: 1436–1444.
- [41] Manera M, Giammarino A, Borreca C, Giari L, Dezfuli BS. Degranulation of mast cells due to compound 48/80 induces concentration-dependent intestinal contraction in rainbow trout (*Oncorhynchus mykiss* Walbaum) ex vivo. *Journal of Experimental Zoology. Part A, Ecological Genetics and Physiology*. 2011; 315: 447–457.
- [42] Giari L, Vincenzi F, Badini S, Guerranti C, Dezfuli BS, Fano EA, et al. Common carp *Cyprinus carpio* responses to sub-chronic exposure to perfluorooctanoic acid. *Environmental Science and Pollution Research International*. 2016; 23: 15321–15330.
- [43] Norušis MJ. Spss® 13.0 Statistical Procedures Companion. Prentice Hall: Upper Saddle River, NJ. 2005.
- [44] Hawkins WE. Ultrastructure of Rodlet Cells: Response to Cadmium Damage in the Kidney of the Spot *Leiostomus xanthurus* Lacépède. *Gulf Res Reports*. 1984; 7: 365–372.
- [45] Vickers T. A Study of the Intestinal Epithelium of the Goldfish *Carassius auratus*: its Normal Structure, the Dynamics of Cell Replacement, and the Changes Induced by Salts of Cobalt and Manganese. *Journal of Cell Science*. 1962; s3–103: 93–110.
- [46] Crivellato E, Nico B, Gallo VP, Ribatti D. Cell secretion mediated by granule-associated vesicle transport: a glimpse at evolution. *Anatomical Record (Hoboken, N.J.: 2007)*. 2010; 293: 1115–1124.